

Fig. S1 VSM curves of GO/Fe<sub>3</sub>O<sub>4</sub>, GO/Fe<sub>3</sub>O<sub>4</sub>-SiO<sub>2</sub> and GO/Fe<sub>3</sub>O<sub>4</sub>-AuNPs

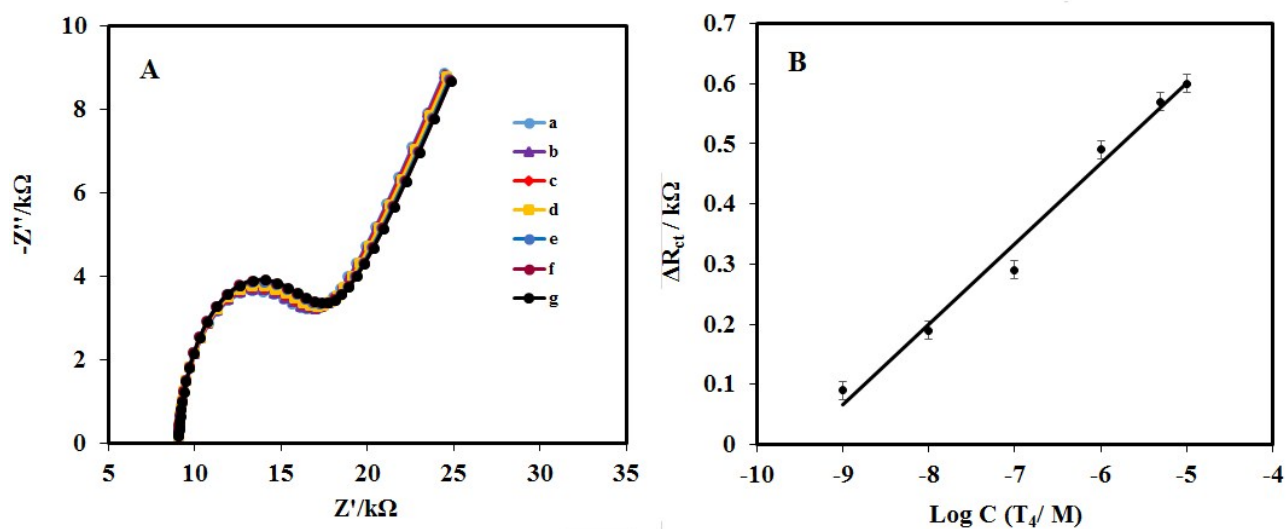


Fig. S2 (A) Nyquist diagrams recorded at (a)  $\text{Fe}_3\text{O}_4/\text{GO-AuNPs}@MIP$  sensor and after loading  $T_4$  in the sites of polymer at different concentrations:  $10^{-9}$ ,  $10^{-8}$ ,  $10^{-7}$ ,  $10^{-6}$ ,  $5 \times 10^{-5}$ ,  $10^{-5}$  M (b-g) respectively, (B) The linear relationship between the  $\Delta R_{ct}$  and the logarithm concentration of  $T_4$ .

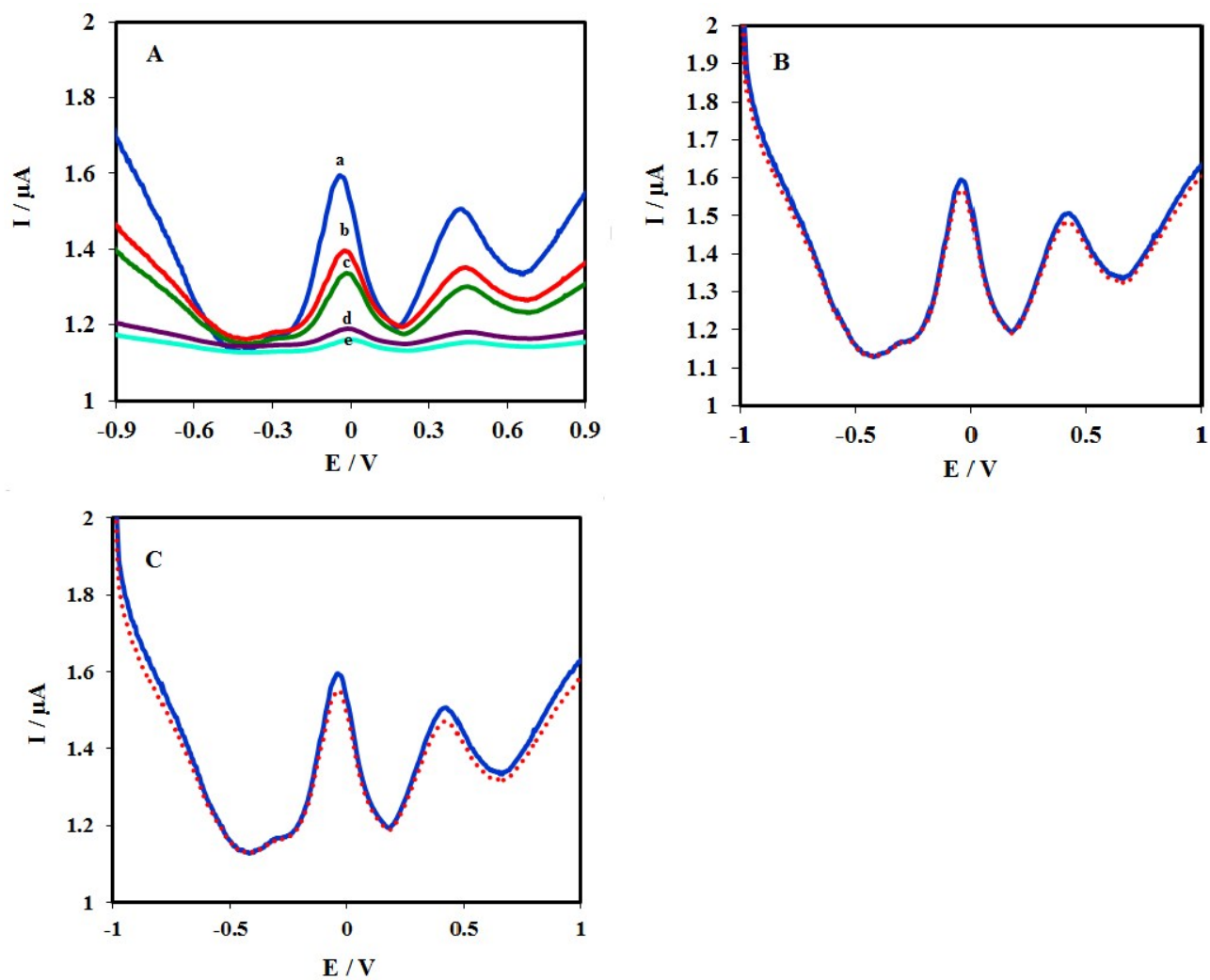


Fig. S3 (A) Current response of (a)  $\text{T}_4$ , (b)  $\text{T}_3$ , (c) Tetrac 1, (d) AA, (e) UA at  $\text{Fe}_3\text{O}_4/\text{GO}-\text{Au}@\text{MIPs}$  electrode, concentration of each compound is  $10^{-7}$  M; (B), (C) Currents of  $\text{Fe}_3\text{O}_4/\text{GO}-\text{AuNPs}@\text{MIPs}$  electrode to  $10^{-7}$  M  $\text{T}_4$  in the presence of  $3 \times 10^{-7}$  M  $\text{T}_3$  and Tetrac 1 respectively.

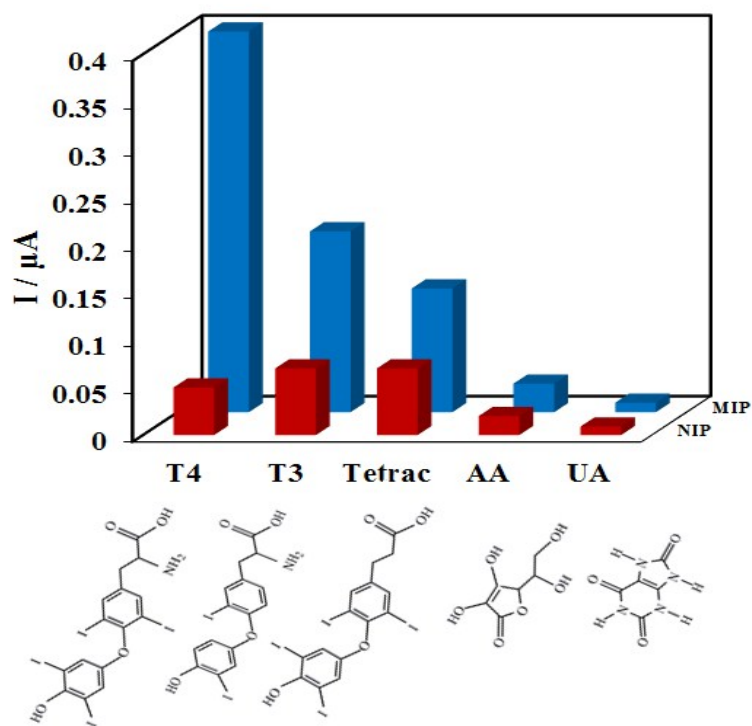


Fig. S4 Selectivity of the MIP and NIP sensor for T<sub>4</sub> and interferences.

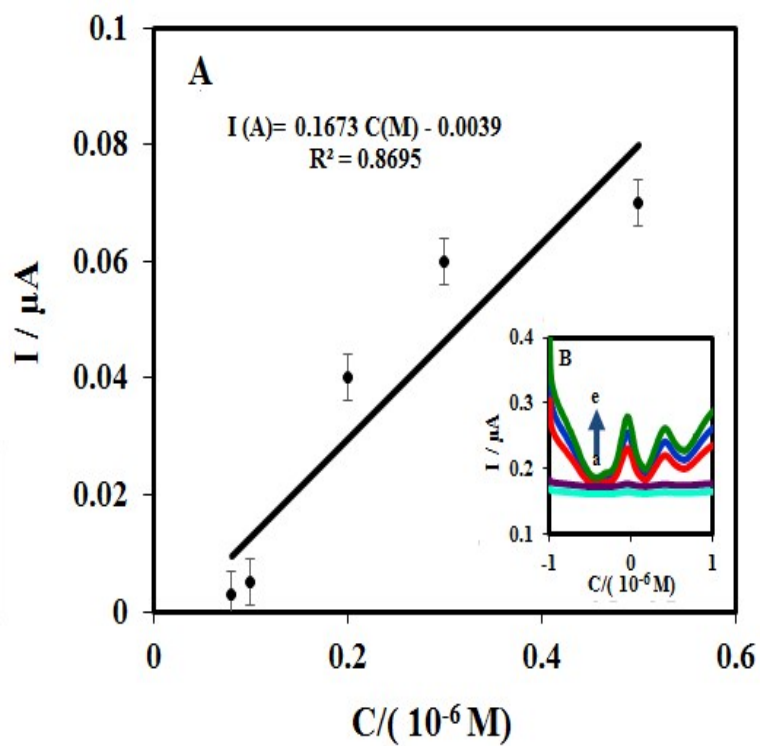


Fig. S5 Calibration curve for concentrations of  $T_4$  with  $Fe_3O_4/GO-AuNPs@NIP$  electrode:  $8 \times 10^{-8}$ ,  $10^{-7}$ ,  $2 \times 10^{-7}$ , (d)  $3 \times 10^{-7}$  and  $5 \times 10^{-7}$  M respectively), (B) DPVs in : (a)  $8 \times 10^{-8}$ , (b)  $10^{-7}$ , (c)  $2 \times 10^{-7}$ , (d)  $3 \times 10^{-7}$ , and (e)  $5 \times 10^{-7}$  M  $T_4$  solution (pH 1.0, scan rate 0.1 V/s).

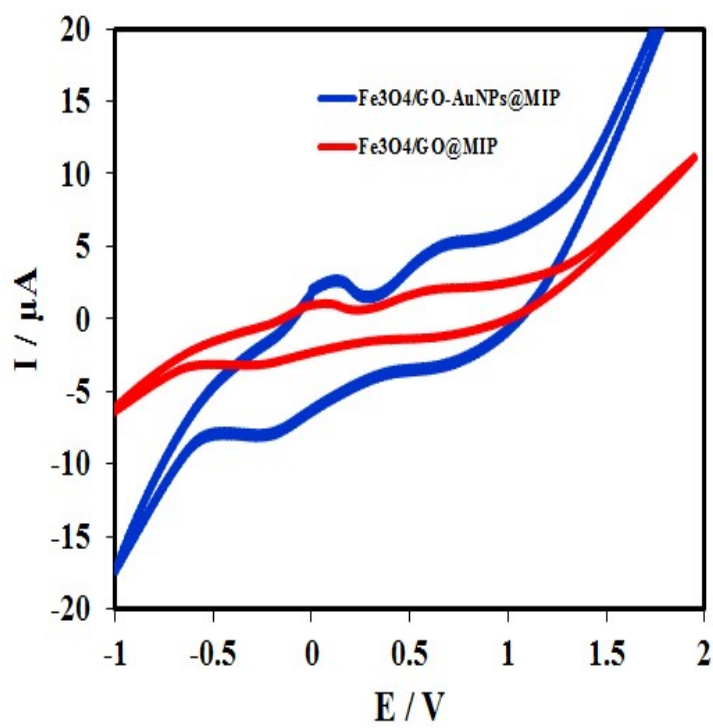


Fig. S6 Cyclic voltammograms for  $10^{-5}$  M  $T_4$  in pH 1.0 obtained at  $Fe_3O_4/GO-AuNPs@MIP$  and  $Fe_3O_4/GO@MIP$  electrodes.